Industrial Engineering Journal
ISSN: 0970-2555
Volume : 53, Issue 10, October : 2024

Mitigation of THD in Grid Connected Inverter using LCL Filter and Adaptive PSO based Controller

[1]T. Pravalika Reddy, PG Student Power Systems
[2]T. Gowri Manohar, Professor in EEE Department
[1, 2]Sri Venkateswara University Tirupati
[1]pravalika3820@gmail.com, [2]gowrimanohart@gmail.com

Abstract:
Three-phase inverters that are connected to the grid are increasingly being used, particularly to provide pure, high-quality current. Full-bridge voltage source inverters are a common form of grid-connected inverter. For smooth and sinusoidal current transmission to the grid, a proportional integral (PI) controller is frequently used. The PI controller can lead to instability in anomalous grid situations, even though it functions effectively in regular grid conditions. Subsequently, the PI controller has begun to be replaced by the proportional resonant (PR) controller in a number of applications, including the regulation of grid-connected currents. A thorough comparison of PI and PR controllers is presented in this paper. Because the PR controller only uses the grid current's positive sequence and only requires one PR controller, the results demonstrate that it reduces total harmonic distortion (THD) and is simpler to implement. This work focusses on using the PR controller because of these reasons. Additionally, an adaptive controller that was modified utilising cutting-edge optimisation methods based on particle swarm optimisation (PSO) was provided in this work. The three-phase grid-connected inverter's control settings are optimised by PSO for both the PR and PI controllers. Using PSO has numerous benefits, one of which is that no new hardware is needed. It is hence extensible to additional applications and control schemes. Furthermore, because the suggested approach self-tunes, it may be appropriate for industrial settings where manual tuning is not advised due to time and expense constraints. A simulation test was run to look into how well the suggested techniques performed.

Keywords- *Grid connected system, LCL filter, PI and PR controller, PLL, Voltage source inverter.*

Introduction:

The rapid depletion of non-renewable resources has resulted in serious problems, including increased pollution and greenhouse gas emissions that raise environmental concerns [1]. Due to its advantages for the environment, distributed power generation (DGs) based on renewable energy has been growing globally in the last few years [2].

Proposed Method:

For a three-phase grid-linked inverter with adaptive PSO, phase-locked loop and LCL filter are used. The signals are generated by PLL and used as a point of reference when the current controller in a grid-connected inverter is implemented [3]. The component that is active is in phase with the alpha signal. Reactive: part that is in sync with the beta signal. The input is DC voltage with a bus capacitor across it. The output of the inverter is then connected to the LCL filter. Lastly, a 3-phase, 3-wire grid connection

Industrial Engineering Journal
ISSN: 0970-2555
Volume : 53, Issue 10, October : 2024

load in a star or delta fashion is connected at the output to implement the controller [4]. The inverter bridge is constructed using a MOSFET or IGBT.

Particle Swarm Optimization:

An adaptive Particle Swarm Optimization (PSO) system is provided herein to control the grid-connected three-phase inverter [5]. PSO is a self-commissioning tuning procedure approach that adjusts the controllers' parameters to handle various normal and abnormal conditions as well as their transitions. PSO is an effective problem-solving approach that can improve system performance [6]. PSO is considerably easier to use and faster to optimise than GA and ANN, which makes it a good fit for real-time control applications that deal with time-varying disturbances [7-8].

A swarm of birds, fish, or bees moving in the search space at a random velocity serves as the inspiration for Particle Swarm Optimisation (PSO), a mathematical technique that produces a particular application of an iterative optimisation technique [9]. The theory of particle location and velocity has served as a representation of the PSO notion.

Here, the best particle among all particles is referred to as the best recorded global position vector, $Xgbestn$, and the best recorded previous position vector is defined as $Xpbestn$ in every iteration [10]. Additionally, the acceleration constants $c1$ and $c2$ are employed, along with τ, an inertia weight that balances the capabilities of "global" and "local" search, and a random value between 0 and 1 [11]. Each particle's position can be changed based on its own local best Pbest and the overall best of the entire swarm population Gbest. Depending on its own local best (Pbest) and the overall best of the entire swarm population (Gbest), each particle may have a different position. Until the predetermined number of iterations is reached, the process continues [12].

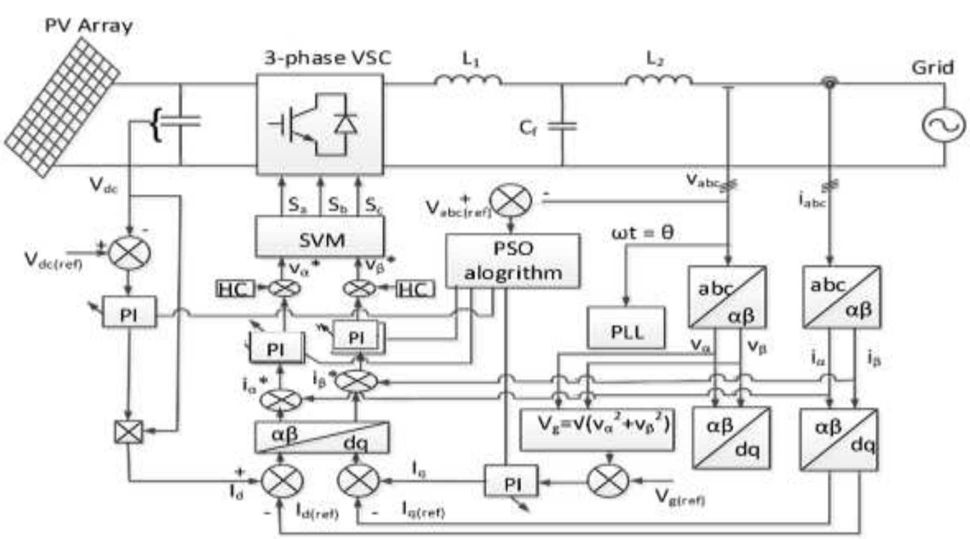

Figure : Network topology of PSO tuned PI controller.

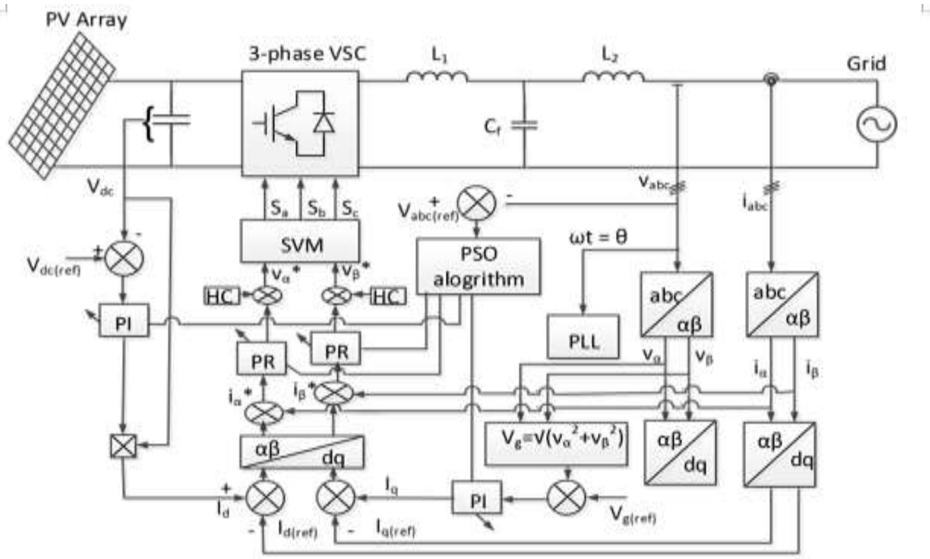

Figure : Network topology of PSO tuned PR controller.

Here, in every iteration, the best recorded previous position vector is defined as, $Xpbestn$, whilst the best particle amongst all particles is referred to as the best recorded global position vector, $Xgbestn$. Also, C_1 and C_2 are acceleration constants, $rand$ is a random value between 0 and 1, and ω is an inertia weight used to balance between 'global' and 'local' search capabilities [13-14]. Depending on its own local best Pbest and the overall best of the entire swarm population Gbest, each particle's position can be modified. Each particle can have a different position depending on its own local best Pbest and the overall best of the entire swarm population Gbest [15]. The procedure keeps going till the specified number of iterations has been reached.

$$V_{id}^{n+1} = \omega . V_{id}^{n} + c_1 . rand . \left(X_{pbest}^{n} - X_{id}^{n}\right) + c_2 . rand . \left(X_{gbest}^{n} - X_{id}^{n}\right)$$

$$X_{i}^{n+1} = X_{id}^{n} + V_{id}^{n+1}$$

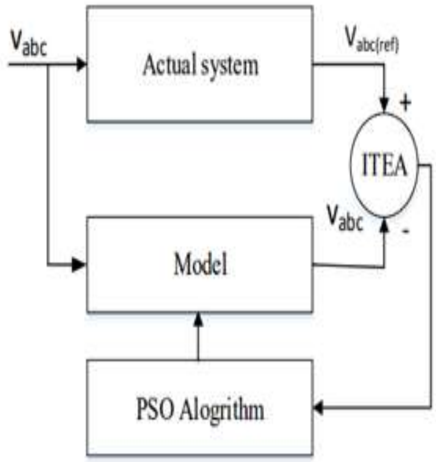

Figure 3: General structure of PSO algorithm

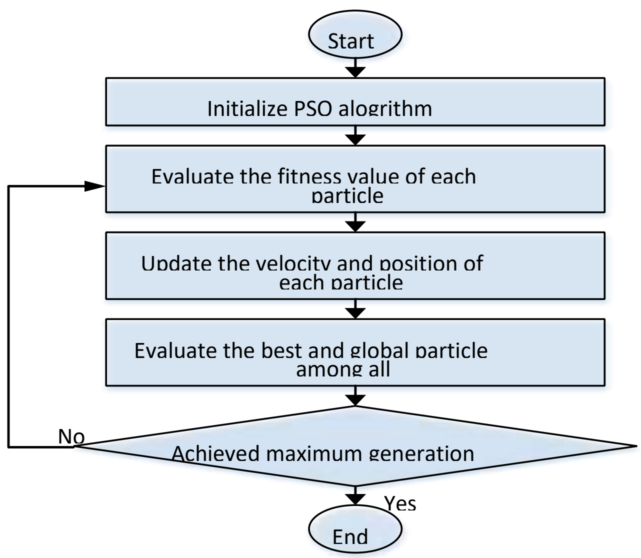

Figure 4: Flowchart of PSO algorithm

Control Parameters for PSO :

The choice of the current control loop has a major impact on the tracking accuracy, steady state error, robust behaviour of the controller, and the dynamic responsiveness of the grid-tied inverter, as Figures 1 and 2 demonstrate [16]. Please see Figures 1 and 2 for an explanation of how PI controllers are used to control DC and grid voltages. PI control loops are used to regulate the grid voltage, DC voltage, and current loops, as can be seen from the control diagram that is shown.

Consequently, the voltage controller outputs are used by d-q current control as its current reference. The three-phase grid current is subjected to this reference before being sent to the appropriate controller. The PI controllers' integral and proportional gains are adjusted using a PSO optimisation technique [17-19]. PSO can also be used in conjunction with a PR controller in a stationary reference frame, as illustrated in

Figure 4. The PSO method is employed in both cases to self-tune the control settings, and the objective function is an integral time absolute error (ITAE) criterion [20].

The voltages and currents in αβ frame are represented as follows:

$$\begin{bmatrix} v_\alpha \\ v_\beta \end{bmatrix} = \frac{2}{3}\begin{bmatrix} 1 & -\frac{1}{2} & -\frac{1}{2} \\ 0 & \frac{\sqrt{3}}{2} & -\frac{\sqrt{3}}{2} \end{bmatrix}\begin{bmatrix} v_a \\ v_b \\ v_c \end{bmatrix} \tag{3}$$

$$\begin{bmatrix} i_\alpha \\ i_\beta \end{bmatrix} = \frac{2}{3}\begin{bmatrix} 1 & -\frac{1}{2} & -\frac{1}{2} \\ 0 & \frac{\sqrt{3}}{2} & -\frac{\sqrt{3}}{2} \end{bmatrix}\begin{bmatrix} i_a \\ i_b \\ i_c \end{bmatrix} \tag{4}$$

Where, v_a,v_b,v_c represent the voltages in 3 phase system while i_a, i_b, i_c represent corresponding currents. Also, v_α, v_β represent voltages and i_α, i_β show the currents in the stationary frame [21]. The voltage magnitude at the point of common coupling (PCC) is expressed as follows:

$$|V_g| = \sqrt{V_{g\alpha}^2 + V_{g\beta}^2} \tag{5}$$

where, vgα and vgβ show grid side voltages. PR controller is represented in the following form:

$$G_{PR}(s) = K_p + K_i \frac{s}{(s^2 + \omega_o{}^2)} \tag{6}$$

The constant Kp represents the proportional term and Ki represents the integral term. Eq. (6) represents an ideal PR controller where the realization of the ideal controller is a challenging task [22]. Thus, the non-ideal PR controller introduced in Eq. (7).

$$G_{PR}(s) = K_p + K_i \frac{2\omega_c s}{(s^2 + 2\omega_c s + \omega_o{}^2)} \tag{7}$$

The calculation of the cost function gives the optimum solution. Integral-based cost functions, such as the Integral Time Absolute Error (ITAE), Integral Square error (ISE) and Integral Time Square Error (ITSE) are commonly utilized [8]. In this research the ITAE approach is implemented as follows.

$$I\,TEA = \int t|(t)|dt \tag{8}$$

Where, e(t) is the difference between the actual value and the reference value. Eq. (1) and Eq. (2) are used to minimize the cost function during the optimization process.

Results and Discussion:

This section presents the simulation results of the three-phase grid-connected system employing PSO optimised controllers. Following each iterative stage of the optimisation procedure, the control parameters are altered. Figure 7 shows the current waveforms using PSO in the synchronous frame of reference, which is based on PI control, whereas Figure 6 shows the three-phase grid voltage. To assess the system's performance under the abnormal grid conditions, the system is specifically designed to withstand the whole 75% voltage sag event during a time span of 0.1 to 0.15 seconds. In order to maintain the flow of active power when the voltage drops, the current must increase. The voltage sag event summarises this process by demonstrating how closely the computed current follows the reference current.

Industrial Engineering Journal

ISSN: 0970-2555

Volume : 53, Issue 10, October : 2024

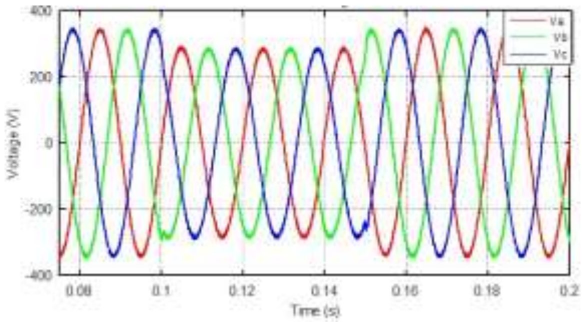

Figure 5. Three-phase voltage waveform using PSO optimized PI control

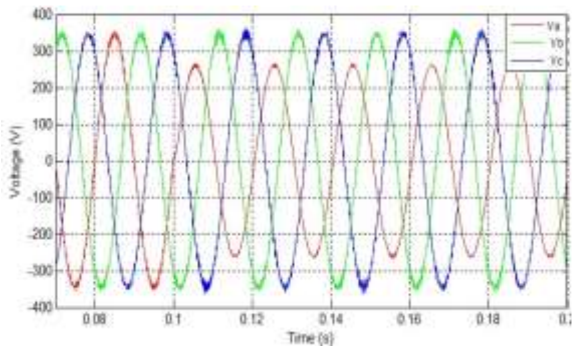

Figure 7. Three-phase voltage waveform using PSO optimized PR control

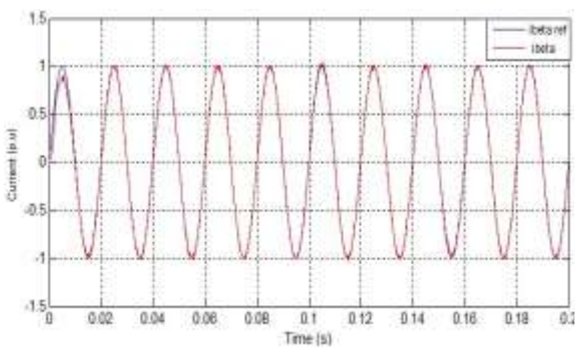

Figure 9. Measured and reference i-alpha using PSO optimized PI control

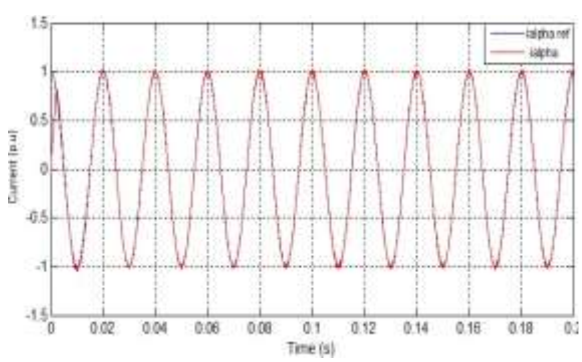

Figure 11. Measured and reference i-alpha using PSO optimized PR control

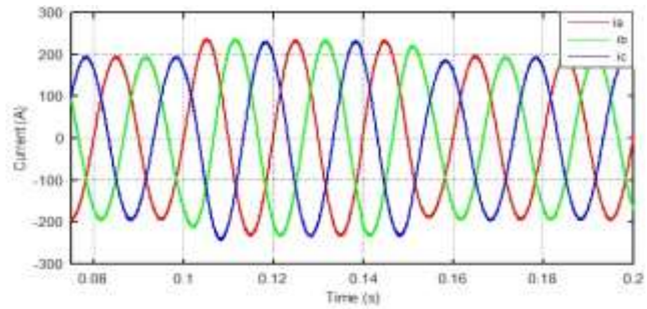

Figure 6. Three-phase current waveform using PSO optimized PI control

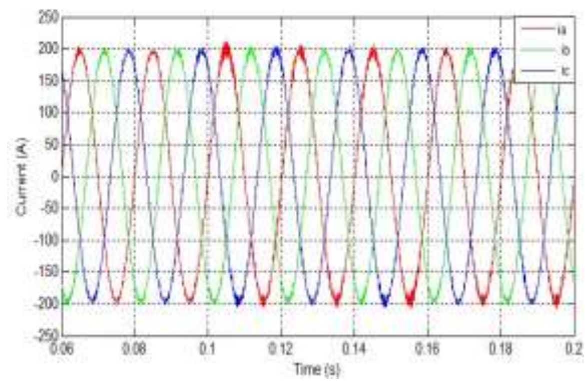

Figure 8. Three-phase current waveform using PSO optimized PR control

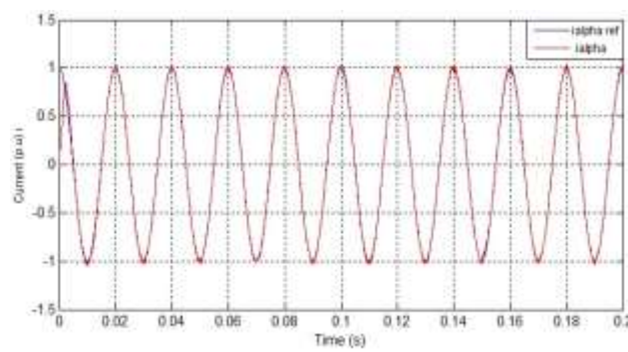

Figure 10. Measured and reference i-beta using PSO optimized PI control

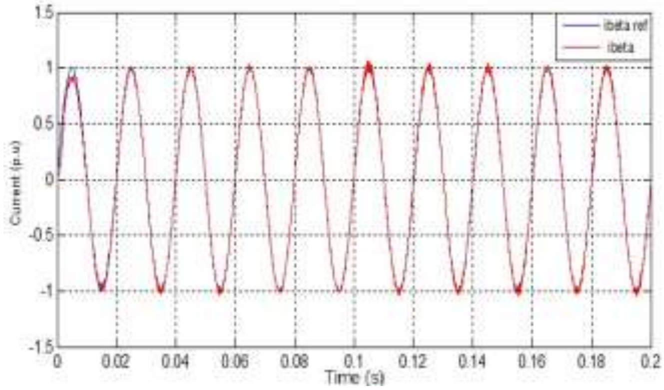

Figure 12. Measured and reference i-beta using PSO optimized PR control

Table : 1. Iteration of the control parameters.

No. of Iterations	K_p	K_i
1	7.812	999.9734
2	7.756	999.965
3	7.361	999.944
4	6.4813	999.8632
5	6.4123	999.8630
6	6.4120	999.7256
7	6.210	999.7112
8	5.4918	999.5735
9	5.4813	999.3682
10	5.4813	999.1632

THD Comparison:

Using PSO-optimized controllers to minimise THD in the current waveforms is one of the work's goals. Figure 13 (a-d) presents the findings. The percentage THD in the grid-injected current waveforms is displayed in Figure 13(a-b) using PI and PR controllers that are conventionally tuned, and in Figure 13(c-d) using PSO-tuned PI and PR controllers, respectively. In the grid injected current waveforms, 3.95% THD is estimated using a typically tuned PI controller, whereas 2.22% THD is recorded using a commonly tuned PR controller. Better performance was demonstrated by PSO-tuned PI and PR controllers, whose estimated THD scores are 2.03% and 1.93%, respectively.

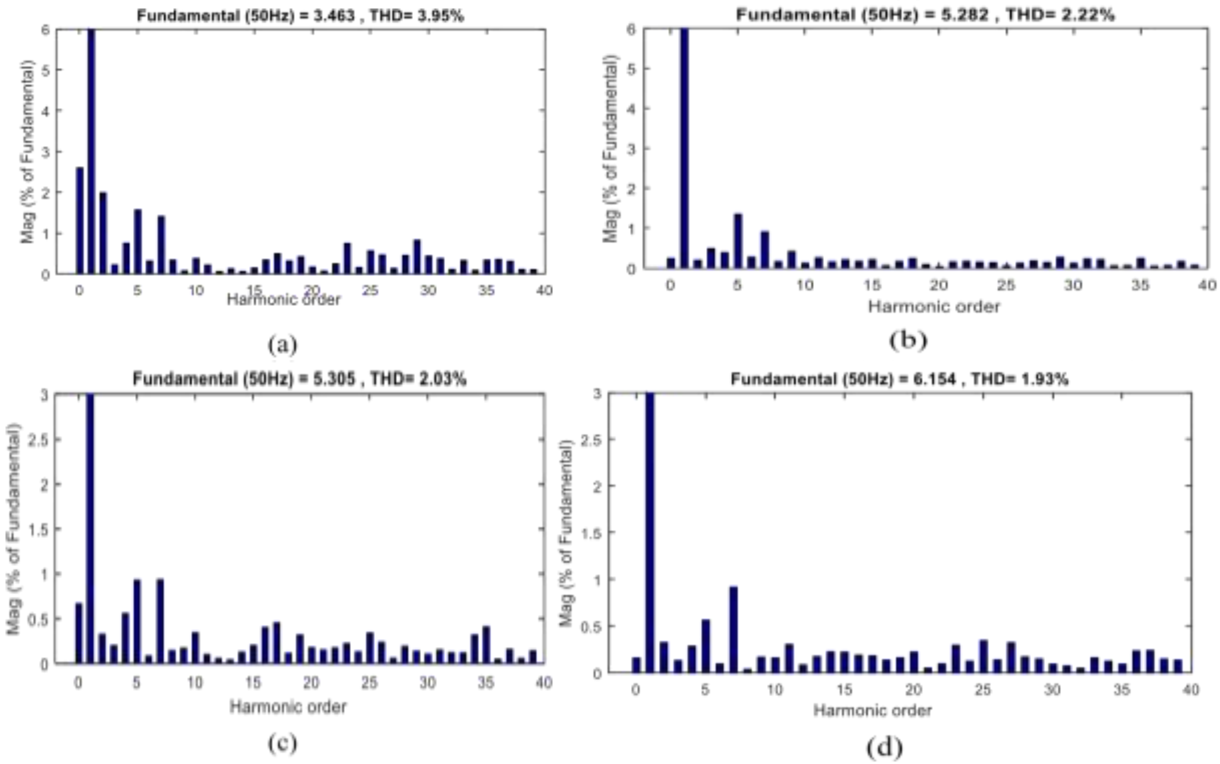

Figure 13. FFT of phase current waveforms: (a) Conventionally tuned PI controller; (b) Conventionally tuned PR controller; (c) PSO tuned PI controller; (d) PSO tuned PR controller

Conclusion:

In this work, the PV integrated grid-tied inverter system's PI and PR controllers were PSOoptimized. The goal of the research is to find a way to reduce the percentage THD score in the injected grid currents. Lower percentage THD scores are specified when using PSO-tuned PI and PR controllers as opposed to traditionally-tuned PI and PR controllers. When the three-phase inverter is linked to the grid under abnormal conditions, there are two major problems with its regulation. Initially, more precise grid synchronisation is needed, and it must be able to handle any current controller in the grid-connected inverter.Second, the reference current generated by the current controller during abnormal conditions has three status levels: balanced, unbalanced, or distorted, and might result in unwanted overcurrent tripping, depending on the desired performance of the three-phase grid-connected inverter. This study presents a simple technique that splits the voltage and current into positive and negative sequence components, respectively. These components are then based on adaptive delayed filters with a one-quarter period deferral. Implementing this filter in MATLAB (Simulink) is the only way to verify its performance in terms of the adaptive control method, which yields good power quality (unity power factor and low THD performance).When compared to PI and PR controllers, the suggested control method can provide shortened total harmonic distortion (THD) in the injected current even when atypical grid conditions exist. The measured current's FFT analysis yields a significantly lower THD value of 1.93%, compared to the traditional PR controller's 2.25% and PI controller's 3.95% THDs. The three-phase grid-connected inverter simulation results show how successful the suggested PSO optimisation strategy is. The findings demonstrated that current THD is decreased to 0.59% with PSO parameter tuning, as opposed to 1.77%

when parameters are adjusted through trial and error. The proposed solution does not require any new hardware and may be implemented without causing a major increase in system complexity and cost.

Future Work:

The effectiveness of the current control methods on the three-phase grid-connected inverter has been examined in this work. Even after a thorough analysis of the effects of unusual grid circumstances, more research is necessary to account for the load resistance in the control .
As a result, the following topics may be of interest for additional research in the future phases of this study: Reactive power compensation is used in voltage regulation under imbalanced settings. The alternative is to use the STATCOM system, which will balance the bus voltage.

References

[1] Afshari, E., Moradi, G.R., Rahimi, R., Farhangi, B., Yang, Y., Blaabjerg, F., Farhangi, S. (2017). Control strategy for three-phase grid-connected PV inverters enabling current limitation under unbalanced faults. IEEE Transactions on Industrial Electronics, 64(11): 8908-8918. https://doi.org/10.1109/TIE.2017.2733481

[2] Bawazir, R.O., Cetin, N.S. (2020). Comprehensive overview of optimizing PV-DG allocation in power system and solar energy resource potential assessments. Energy Reports, 6: 173-208. https://doi.org/10.1016/j.egyr.2019.12.010

[3] Benz, C.H., Franke, W.T., Fuchs, F.W. (2010). Low voltage ride through capability of a 5 kW grid-tied solar inverter. In Proceedings of 14th International Power Electronics and Motion Control Conference EPE-PEMC 2010, pp. T12-13. https://doi.org/10.1109/EPEPEMC.2010.5606829

[4] Ueda, Y., Kurokawa, K., Kitamura, K., Yokota, M., Akanuma, K., Sugihara, H. (2009). Performance analysis of various system configurations on grid-connected residential PV systems. Solar Energy Materials and Solar Cells, 93(6-7): 945-949.https://doi.org/10.1016/j.solmat.2008.11.021

[5] Borni, A., Abdelkrim, T., Bouarroudj, N., Bouchakour, A., Zaghba, L., Lakhdari, A., Zarour, L. (2017). Optimized MPPT controllers using GA for grid connected photovoltaic systems, comparative study. Energy Procedia, 119: 278-296. https://doi.org/10.1016/j.egypro.2017.07.084

[6] Buzo, R.F., Barradas, H.M., Leão, F.B. (2021). Fault current of PV inverters under grid-connected operation: A review. Journal of Control, Automation and ElectricalSystems,32(4): 1053-1062. https://doi.org/10.1007/s40313-021-00729-6

[7] Chine, W., Mellit, A., Pavan, A.M., Kalogirou, S.A. (2014). Fault detection method for grid-connected photovoltaic plants. Renewable Energy, 66: 99-110. https://doi.org/10.1016/j.renene.2013.11.073

[8] Ali Khan, M.Y., Liu, H., Yang, Z., Yuan, X. (2020). A comprehensive review on grid connected photovoltaic inverters, their modulation techniques, and control strategies. Energies, 13(16): 4185.https://doi.org/10.3390/en13164185

[9] Díez-Mediavilla, M., Dieste-Velasco, M.I., RodríguezAmigo, M.D.C., García-Calderón, T., Alonso-Tristán, C. (2014). Performance of grid-tied PV facilities based on real data in Spain: Central inverter versus string system. Energy Conversion and Management, 86: 1128-1133. https://doi.org/10.1016/j.enconman.2014.06.087

[10] Bacha, S., Picault, D., Burger, B., Etxeberria-Otadui, I., Martins, J. (2015). Photovoltaics in microgrids: An overview of grid integration and energy management aspects. IEEE Industrial Electronics Magazine, 9(1): 33-46. https://doi.org/10.1109/MIE.2014.2366499

[11] Guenounou, O., Belkaid, A., Colak, I., Dahhou, B., Chabour, F. (2021). Optimization of fuzzy logic controller based maximum power point tracking using hierarchical genetic algorithms. In 2021 9th International Conference on Smart Grid (icSmartGrid), pp. 207-211. https://doi.org/10.1109/icSmartGrid52357.2021.9551249

[12] Guerrero-Perez, J., De Jodar, E., Gómez-Lázaro, E., Molina-Garcia, A. (2014). Behavioral modeling of gridconnected photovoltaic inverters: Development and assessment. Renewable Energy, 68: 686-696. https://doi.org/10.1016/j.renene.2014.02.022

[13] Gui, Y., Wang, X., Blaabjerg, F. (2018). Vector current control derived from direct power control for gridconnected inverters. IEEE Transactions on PowerElectronics, 34(9): 9224-9235.https://doi.org/10.1109/TPEL.2018.2883507

[14] Chuang, M., Hong, L. (2019). Research on photovoltaic grid-connected control of Z source inverter based on active disturbance rejection technology. In 2019 IEEE 4th Advanced Information Technology, Electronic and Automation Control Conference (IAEAC), 1: 2648-2652.https://doi.org/10.1109/IAEAC47372.2019.8997945

[15] Bhagiya, R.D., Patel, R.M. (2019). PWM based double loop PI control of a bidirectional DC-DC converter in a standalone PV/battery DC power system. In 2019 IEEE 16th India council international conference (INDICON), pp. 1-4. https://doi.org/10.1109/INDICON47234.2019.9028974

[16] Yadav, A., Chandra, S. (2020). Single stage high boost Quasi-Z-Source inverter for off-grid photovoltaic application. In 2020 International Conference on Power Electronics & IoT Applications in Renewable Energy and its Control (PARC), pp. 257-262. https://doi.org/10.1109/PARC49193.2020.236603

[17] Mohammed, F.A., Bahgat, M.E., Elmasry, S.S., Sharaf, S.M. (2022). Design of a maximum power point tracking-based PID controller for DC converter of standalone PV system. Journal of Electrical Systems andInformation Technology, 9(1): 9.https://doi.org/10.1186/s43067-022-00050-5

[18] Chamundeeswari, V., Seyezhai, R. (2017). PSO-PID maximum power point tracking controller using modified superlift Luo converter. Energy Procedia, 117: 87-94. https://doi.org/10.1016/j.egypro.2017.05.110

[19] Banakhr, F.A., Mosaad, M.I. (2021). High performance adaptive maximum power point tracking technique for off-grid photovoltaic systems. Scientific Reports, 11(1): 20400. https://doi.org/10.1038/s41598-021-99949-8 [20]Hassan, Z., Amir, A., Selvaraj, J., Rahim, N.A. (2020). A review on current injection techniques for low-voltage ride-through and grid fault conditions in grid-connected photovoltaic system. Solar Energy, 207: 851-873. https://doi.org/10.1016/j.solener.2020.06.085

[21] Borni, A., Bouarroudj, N., Bouchakour, A., Zaghba, L. (2017). P&O-PI and fuzzy-PI MPPT controllers and their time domain optimization using PSO and GA for gridconnected photovoltaic system: A comparative study. International Journal of Power Electronics, 8(4): 300-322. https://doi.org/10.1504/IJPELEC.2017.085199

[22] Gui, Y., Wang, X., Blaabjerg, F., Pan, D. (2019). Control of grid-connected voltage-source converters: The relationship between direct-power control and vectorcurrent control. IEEE Industrial Electronics Magazine, 13(2): 31-40.https://doi.org/10.1109/MIE.2019.2898012.